THE JOURNAL OF PHYSICAL CHEMISTRY B

ARTICLE

pubs.acs.org/JPCB

First-Principles Calculations of Structural, Elastic, Electronic, and Optical Properties of Perovskite-type $KMgH_3$ Crystals: Novel Hydrogen Storage Material

Ali H. Reshak,*[,†,‡] Mikhail Y. Shalaginov,[§] Yasir Saeed,[†] I. V. Kityk,[∥] and S. Auluck[⊥,#]

[†]Institute of Physical Biology, South Bohemia University, Nove Hrady 37333, Czech Republic

[‡]School of Microelectronic Engineering, University Malaysia Perlis (UniMAP), Block A, Kompleks Pusat Pengajian, 02600 Arau Jejawi, Perlis, Malaysia

[§]School of Electrical and Computer Engineering, Purdue University, West Lafayette, 47907 Indiana, United States

[∥]Electrical Engineering Department, Technical University of Czestochowa, Al.Armii Krajowej 17/19, Czestochowa, Poland

[⊥]Physics Department, Indian Institute of Technology Kanpur, Kanpur (UP) 208016, India

[#]National Physical Laboratory Dr. K S Krishnan Marg, New Delhi 110012, India

ABSTRACT: We report a first-principles study of structural and phase stability in three different structures of perovskite-types $KMgH_3$ according to H position. While electronic and optical properties were measured only for stable perovskite-type $KMgH_3$, our calculated structural parameters are found in good agreement with experiment and other theoretical results. We also study the electronic charge density space distribution contours in the (200), (101), and (100) crystallographic planes, which gives better insight picture of chemical bonding between K−H, K−Mg−H, and Mg−H. Moreover, we have calculated the electronic band structure dispersion, total, and partial density of electron states to study the band gap origin and the contribution of s-band of H, s and p-band of Mg in the valence band, and d-band of K in the conduction band. Furthermore, optical features such as dielectric functions, refractive indices, extinction coefficient, optical reflectivity, absorption coefficients, optical conductivities, and loss functions of stable $KMgH_3$ were calculated for photon energies up to 40 eV.

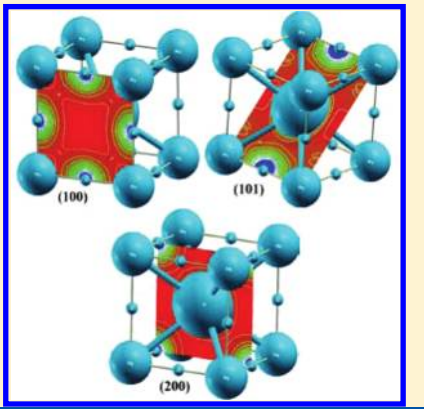

1. INTRODUCTION

In recent years, one can observe an enhanced interest to groups I−III of the periodic table, for example, K, Li, Na, Mg, Ba, Sr, and Al, to form different types of complex hydrides that are interesting for the use as potential hydrogen storage materials because of their light weight. Today a lot of research activity is in progress with the aim to identify new materials with high hydrogen content and suitability to functionalize at low operating temperature.

Perovskite hydrides ABH_3 are gaining much interest because of cubic structure and presence of lightweight elements like $CsCaH_3$, $RbCaH_3$, $KMgH_3$, $BaLiH_3$, and $SrLiH_3$.[1−4] Mg-based phases receive particular attention because of lightweight and low cost production. Recently, a number of theoretical studies were carried out for structural and electronic properties in different phases of $MMgH_3$ (M = Li, Na, K, Rb, Cs).[5,6] For hydrides, owing to the complexity in structural arrangements and difficulties involved in establishing hydrogen positions by X-ray diffraction methods, structural information is limited.[7] However, most of these materials are not well-described and thermodynamic data are absent.[8] Some of theoretical results are available only for the stability of these perovskite hydrides $XLiH_3$ (X = Ba and Sr)[9] and XCaH3 (X = Cs and Rb)[10] under pressure. But for Mg-based perovskite hydride $KMgH_3$, no experimental or theoretical data for phase stability related to hydrogen positions are available. Keeping these points in view, we focus on stability of perovskite-type $KMgH_3$ according to different hydrogen positions and investigate the electronic and optical properties in that stable phase only.

In the next section, we briefly describe the calculation procedure and give the Computational Details. In Section 3, we report and discuss our result for structural and phase stability of three different phases and then present the electronic and optical properties of only stable phase $KMgH_3$. Finally, conclusions will be given in Section 4.

2. COMPUTATIONAL DETAILS

Ab initio calculations for different phases of perovskite-type $KMgH_3$ are performed using the full potential linearized augmented plane wave plus local orbitals (FP-LAPW + lo) method within a framework of density functional theory (DFT), as implemented in the WIEN2K code.[11] The generalized gradient approximation (GGA)[12] was used for the exchange-correlation potential. In these calculations, FP-LAPW + lo basis set consisted of $3p^6$, $4s^1$ states of K, $2p^6$, $3s^2$ states of Mg, and $1s^1$ state of H.

Received: November 30, 2010

dx.doi.org/10.1021/jp111382h | *J. Phys. Chem. B* XXXX, XXX, 000–000

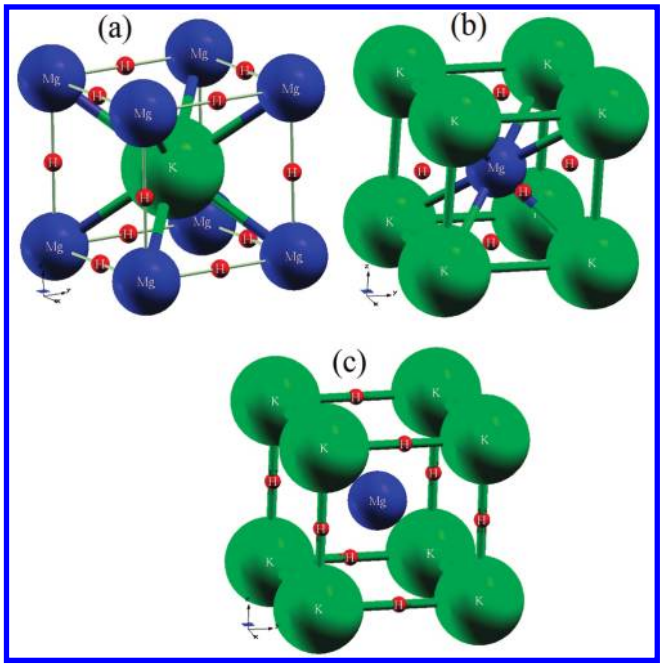

Figure 1. Crystal structures of $KMgH_3$ (a) **Stable** (b) **US1**, and (c) **US2**.

The unit cell was divided into two regions. The spherical harmonic expansion was used inside the nonoverlapping spheres of muffin-tin radius (R_{mt}) and the plane wave basis set was chosen in the interstitial region (IR) of the unit cell. The R_{mt} for K, Mg, and H were chosen in such a way that the spheres did not overlap. To get the total energy convergence, the basis functions in the IR were expanded up to $R_{mt} \times K_{max} = 6.0$ and inside the atomic spheres for the wave function. The maximum value of l were taken as $l_{max} = 10$, while the charge density is Fourier expanded up to $G_{max} = 18$ (au)$^{-1}$. We have used 35 k-points in the irreducible Brillouin zone for structural optimization. For electronic properties calculation 84 k-points were used. A denser sampling of the BZ was required to calculate the optical properties of the samples. A mesh of 220 k-points was used for the optical calculations.

3. RESULTS AND DISCUSSION

3.1. Structural Properties and Phase Stability. The perovskite-type $KMgH_3$ crystals possess the space group $Pm\bar{3}m$. The structural properties and phase stability of three different phases of perovskite-type $KMgH_3$ are the following: first, the structure unstable-$KMgH_3$ (**US1**) with atomic position K (0, 0, 0), Mg (1/2, 1/2, 1/2), and H (0, 1/2, 1/2) given in ref 5; second, the unstable-$KMgH_3$ (**US2**) with atomic position K (0, 0, 0), Mg (1/2, 1/2, 1/2), and H (1/2, 0, 0),; and third, the stable-$KMgH_3$ (**Stable**) with atomic position Mg (0, 0, 0), K (1/2, 1/2, 1/2), and H (1/2, 0, 0) like BaLiH3[9] as shown in Figure 1.

First, we calculate the total energy versus unit cell volume of these phases as shown in Figure 2. The **US1** and **Stable** phases are energetically very close but **US1** phase has lower ground-state energy with respect to **US2** and the **Stable** phase. The equilibrium lattice constant a, bulk modulus B, the derivative of the bulk modulus B' and nearest neighbor (nn) bond length distances using GGA approximation are listed in Table 1. These results have been obtained by fitting the calculated total energies to

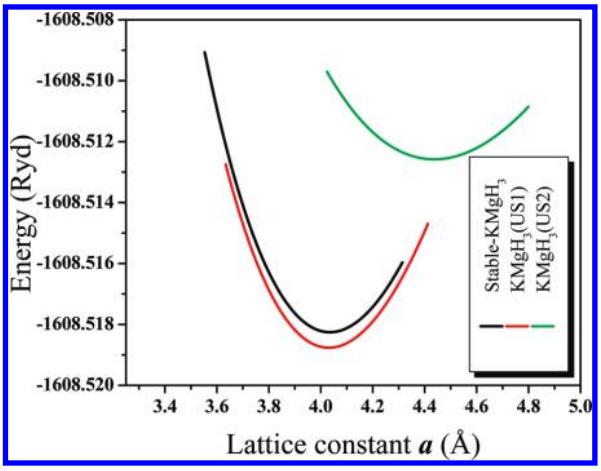

Figure 2. Comparison of total energy versus lattice constants for different phases of $KMgH_3$ with PBE-GGA approximation.

Murnaghan equation of state.[13] The calculated unit cell parameters of **US1** and the **Stable** phase are in good agreement with available experimental and theoretical results. However, the **US2** phase predicts higher lattice constant and lower bulk modulus compared to other phases of KMgH3. In both **US1** and **Stable** phase, K is surrounded by 12 H at distance of 2.85 Å and Mg is octahedral coordinated by 6 H at distance of 2.02 Å. The shortest H−H bond length distance is 2.85 Å. While in **US2** phase, Mg is surrounded by 12 H at distance of 3.318 Å and K is octahedral coordinated by 6 H at distance 2.219 Å. The shortest H−H bond length distance is 3.138 Å.

To investigate the phase stability of these phases taking into account different H positions, we study the elastic properties using the Mehl method.[14] The cubic structure is mainly characterized by three independent elastic constants: C_{11}, C_{12}, and C_{44}. The present values of elastic constants of **US1**, **US2**, and **Stable** $KMgH_3$ phase are listed in Table 1. For a cubic crystal, its mechanical stability requires that its three independent elastic constants should satisfy the following relations[15]

$$(C_{11} - C_{12}) > 0, \quad C_{11} > 0, \quad C_{44} > 0, \quad (C_{11} + 2C_{12}) > 0 \tag{1}$$

These conditions also lead to a restriction on the magnitude of B

$$C_{12} < B < C_{11} \tag{1a}$$

The predicted C_{ij} values (see Table 1) for **US1**, **US2**, and **Stable** $KMgH_3$ satisfy all above conditions, except $C_{44} > 0$, which have values of −24.4, −18.9, and 34.733 for **US1**, **US2**, and **Stable** phase, respectively.

In these three phases, the **Stable** $KMgH_3$ is the only phase that matches all the conditions necessary for stable structure. Thus our calculated elastic study indicates that cubic perovskite-type **Stable** $KMgH_3$ phase is mechanically stable. To the best of our knowledge, values of elastic constants have not yet measured experimentally and theoretically for this compound. Hence our results can help to plan future experiments to investigate the stability of $KMgH_3$.

3.2. Electronic Space Charge Density Distribution. We have investigated the two-dimensional (2D) electronic charge density contours in the (200), (101), and (100) crystallographic planes of perovskite-type **Stable** $KMgH_3$ to analyze the origin of chemical bonds between all atoms K−H, K−Mg−H, and M−H

dx.doi.org/10.1021/jp111382h |J. Phys. Chem. B XXXX, XXX, 000–000

Table 1. Atomic Coordinates (K, Mg, H) Calculated Lattice Constants a (Å), Bulk Modulus B_0 (GPa), Derivative of Bulk Modulus B'_0, Elastic Constants (GPa), Nearest Neighbor Bond Length Distances (Å), and Indirect Band Gap E_g (eV) for US1, US2, and Stable Phase of $KMgH_3$ Compared with Available Other Theoretical and Experimental Results

$KMgH_3$	US1	US2	Stable	other theoretical	experiment
			atomic coordinates		
K	(0 0 0)	(0 0 0)	(0.5 0.5 0.5)	(0 0 0)[b,c]	(0 0 0)[d]
Mg	(0.5 0.5 0.5)	(0.5 0.5 0.5)	(0 0 0)	(0.5 0.5 0.5)[b,c]	(0.5 0.5 0.5)[d]
H	(0.5 0.5 0)	(0.5 0 0)	(0.5 0 0)	(0.5 0.5 0)[b,c]	(0.5 0.5 0)[d]
a	4.034	4.44	4.035	4.0295[b], 4.01[c]	4.023[a], 4.025[d]
B_0	34.805	21.08	35.1008	35.6[b]	
B'_0	3.77	4.19	3.57	3.7[b]	
C_{11}	55.073	46.189	75.076		
C_{12}	8.684	19.723	19.752		
C_{44}	−24.438	−18.899	34.733		
			nn bond length distances		
K−H	2.85	2.219	2.853	2.85[b]	
K−Mg	3.49	3.843	3.495	3.49[b]	
Mg−H	2.02	3.138	2.018		
H−H	2.85	3.138	2.853		
E_g (X−R)	2.23		2.53	2.32[b],2.6[e]	

[a] Reference 16. [b] Reference 5. [c] Reference 17. [d] Reference 3. [e] Reference 6.

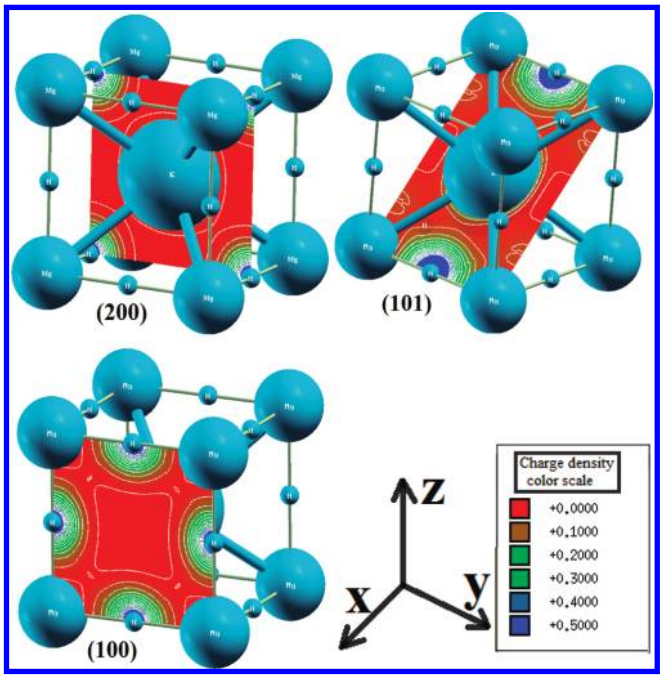

Figure 3. Calculated electronic charge densities of stable-$KMgH_3$ in (200), (101), and (100) planes along with arbitrary color scale.

as shown in Figure 3. In the (200) plane, it is found that majority of charges are accumulated on H site and the distribution of electronic charge is spherical which results in the bonding between K−H showing prevailingly ionic features because the large electronegativity difference between K (0.82) and H (2.1). Also in (100) plane, H forms ionic bonding with Mg (Pauling electronegativity = 1.31) and charge distribution around Mg is not spherical. This is probably because of Mg-s and -p state contribution to valence band. Charge contour plot along (101) plane shows collective behavior between all atoms like K−Mg−H. Moreover, this plot shows that valence electrons from K and Mg sites are transferred to H site, which is also predicted by VASP calculation in ref 5 for **US1** phase. This can be seen easily by color charge density scale where blue color (+0.5000) corresponds to the maximum charge accumulation site.

3.3. Electronic Band Structure and Density of States. The electronic band structure of perovskite-type $KMgH_3$ in all three phases are shown in Figure 4 along the high symmetry directions in the irreducible Brillouin zone. The **US1** and **Stable** phase show similar band structure dispersions in k-space with wide indirect band gaps (E_g) 2.23 and 2.53 eV, respectively, along X−R symmetry, while **US2** phase shows a metallic behavior in contrast with the semiconductor nature of **US1** and **Stable** phase. Here we will pay more attention on the comparison between the band diagram of **US1** and **Stable** phase. We should emphasize that by changing the position of H from (0.5 0.5 0) to (0.5 0 0) as well as replacing K by Mg, the electronic properties are not affected at all. That is why in further study we only consider the **Stable** $KMgH_3$. The valence band near the Fermi level is basically originated from H s-band with a small admixture of Mg, which leads to the dependency of band energy versus number of H atoms in unit cell, whereas the majority part of the conduction band is caused by d-band of K. The calculated values of the energy gaps (E_g) are listed in Table 1.

To understand the effect of atomic relaxation on the electronic band structure, we calculate the total density of states (TDOS) and partial density of states (PDOS) for perovskite-type $KMgH_3$ crystals as shown in Figure 5. The results of TDOS show that **Stable** $KMgH_3$ exhibits wide band gap features possessing the value equal to about 2.53 eV, which is not the traditional semiconductor but uses it as a potential source for hydrogen storage material because all the valence bands are occupied by the H s-state from 0 to −5.568 eV as shown in TDOS and PDOS of H. There exists a local orbital in TDOS at semicore level situated around −12.262 eV that is almost completely originated from K p-state. The conduction band from 2.53 up to 20.0 eV is

dx.doi.org/10.1021/jp111382h |J. Phys. Chem. B XXXX, XXX, 000–000

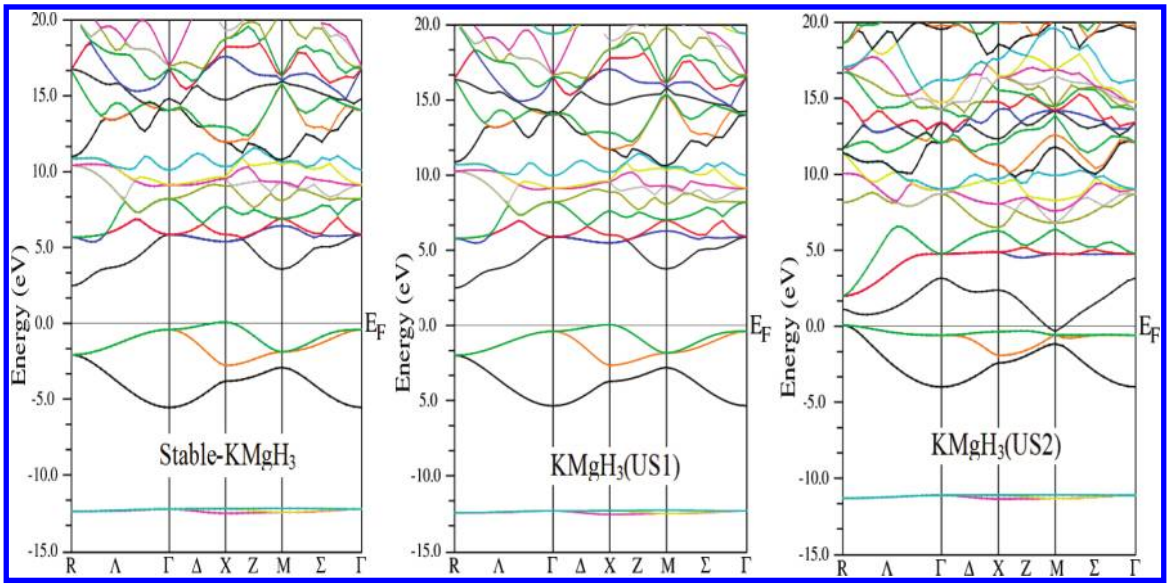

Figure 4. Calculated high-symmetry band structures for $KMgH_3$ in **Stable**, **US1**, and **US2** phase.

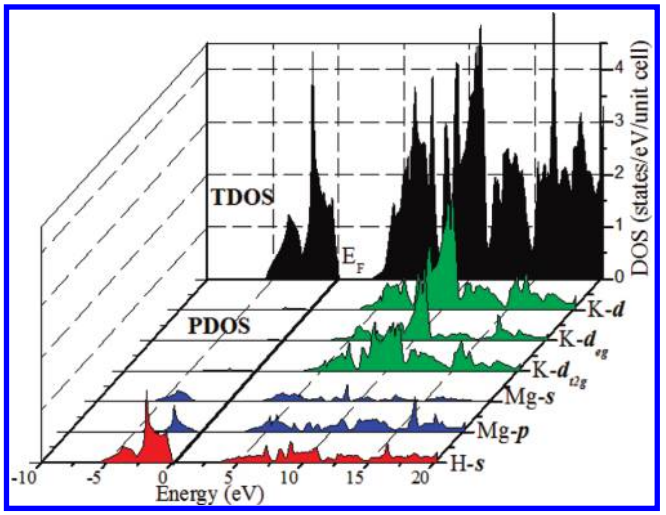

Figure 5. Calculated TDOS of **Stable** $KMgH_3$ and PDOS of Mg-s, Mg-p, K-p, K-d_{eg}, K-d_{t2g} and H-s states contribution in TDOS.

dominant by K d-state where d-state also split due to crystal field hybridizatizon into d_{eg} and d_{t2g} substates which are clearly observed in PDOS of K (see Figure 5). One can notice that the Mg atom has very small contribution to conduction band as well as to valence band originating from its s- and p-states. Mg-s and -p states are energetically well separated in valence band but partially degenerated in conduction band region. For our calculated **Stable** phase, the TDOS and PDOS are in good agreement with those obtained for **US1** phase by other theoretical work.[5]

3.4. Dispersion of Optical Susceptibilities. The frequency dependent dielectric function (dispersion of dielectric function) $\varepsilon(\omega) = \varepsilon_1(\omega) + i\varepsilon_2(\omega)$ is used to describe the linear optical properties. The equation of the frequency dependent imaginary part of a dielectric function $\varepsilon_2(\omega)$ for cubic crystal as given in ref 18 is

$$\varepsilon_2(\omega) = \frac{8}{2\pi\omega^2}\sum|P_n(k)|^2\frac{dS_k}{\nabla\omega_n(k)} \qquad (2)$$

where $P_n(k)$ is the outerband transition dipole momentum matrix. The dielectric function, $\varepsilon_2(\omega)$, is strongly correlated to the joint density of states (DOS) and transition momentum matrix elements. The real part of the dielectric function $\varepsilon_1(\omega)$ can be obtained from $\varepsilon_2(\omega)$ by Kramers−Kronig relation as given in ref 19 is

$$\varepsilon_1(\acute{\omega}) = \frac{2}{\pi}P\int_0^{\infty}\frac{\acute{\omega}\,\varepsilon_{2(\acute{\omega})}}{\acute{\omega}^2 - \omega^2}\,\mathrm{d}\,\acute{\omega} \qquad (3)$$

Using the dispersion of real and imaginary parts of dielectric functions one can calculate dispersion of other optical parameters such as refractive indices, reflectivity, optical conductivities, absorption coefficientand so forth.

The linear optical susceptibility of **Stable** $KMgH_3$ has been investigated by calculating the optical parameters, dielectric function $\varepsilon(\omega)$, refractive index (n), extinction coefficient (k), reflectivity $R(\omega)$, absorption coefficient $I(\omega)$, optical conductivity $\sigma(\omega)$ and electron energy-loss function $L(\omega)$. The dispersion of the real and imaginary parts of dielectric function, $\varepsilon_1(\omega)$ and $\varepsilon_2(\omega)$, for **Stable** $KMgH_3$ are shown in Figure 6a. The analysis of $\varepsilon_2(\omega)$ spectra shows the threshold energy occurring at 2.62 eV, which correspond to the indirect optical transition between highest valence H-s originated band and lowest conduction Mg-s bands. It is clear from the figure that $\varepsilon_2(\omega)$ shows three major energy spectral peaks situated at 5.53 (principal peak), 7.76, and 23.04 eV. The highest peak in $\varepsilon_2(\omega)$ at 5.53 eV is 11.49, corresponds to the transition from occupied H-s to unoccupied Mg-s band states. The static dielectric constant $\varepsilon_1(0)$ without any contribution from lattice vibration is equal to about 3.74. We should emphasize that wide band energy gap yields a smaller value of $\varepsilon_1(0)$. This is inversely proportional property could be understand within a framework of Penn model expression;[20] $\varepsilon_1(0) \approx 1 + (\hbar\omega_p/E_g)^2$. First main and highest peak value 10.79 of $\varepsilon_1(\omega)$ exists at energy 5.10 eV, while all other peaks have negative value −1.03, −1.06, and −0.67 at energies 8.61, 6.76, and 23.41 eV, respectively.

The calculated static refractive index $n(0)$ is equal to 1.93 while $n(\omega)$ and $k(\omega)$ have maximum values at 5.23 and 5.7 eV, respectively, as shown in Figure 6b. In Figure 6c, the maximum of reflectivity (0.40 or 40%) is at about 23.58 eV (λ = 52.6 nm),

dx.doi.org/10.1021/jp111382h |J. Phys. Chem. B XXXX, XXX, 000–000

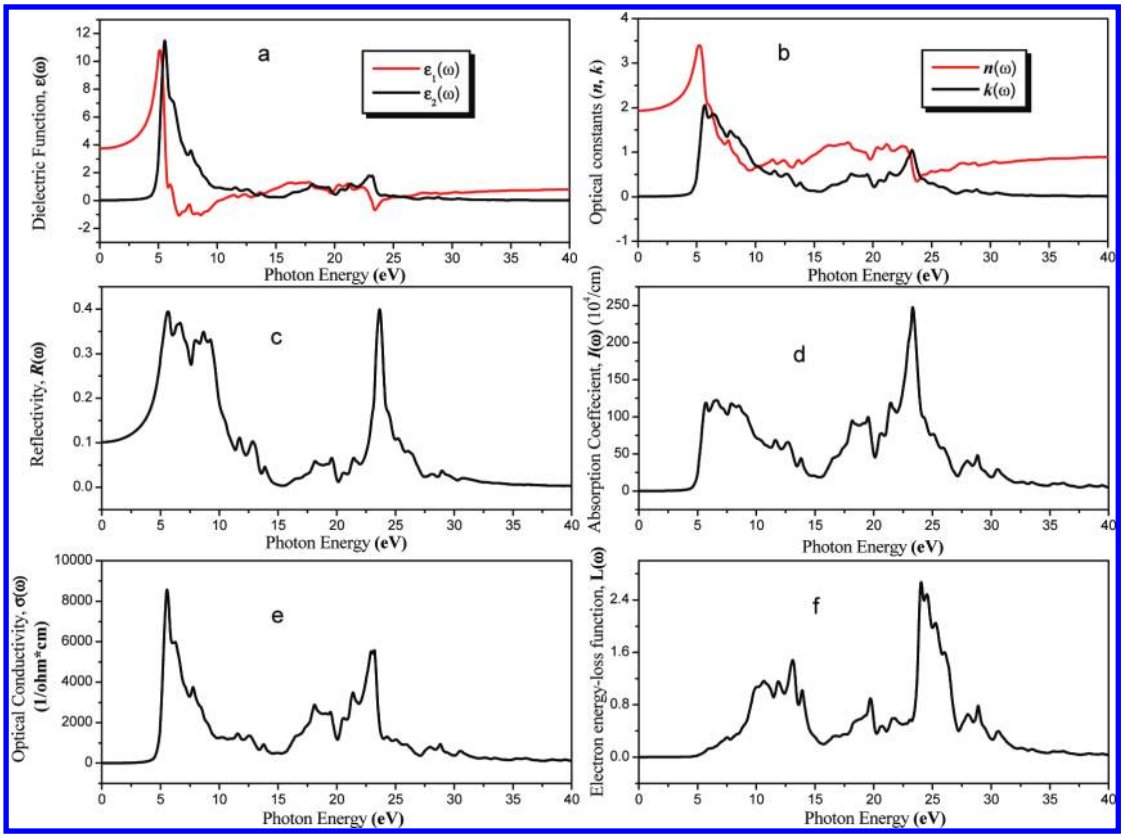

Figure 6. The calculated optical properties of stable $KMgH_3$ (a) Dielectric function $\varepsilon(\omega)$, (b) optical constant (n, k), (c) reflectivity $R(\omega)$, (d) absorption coefficient $I(\omega)$, (e) optical conductivity $\sigma(\omega)$, (f) electron energy-loss function $L(\omega)$.

which is in UV region. Therefore the **Stable** $KMgH_3$ can be considered as shielding from UV radiations. Also the reflectivity has peaked close to maximum with value 0.3935 at 5.57 eV (λ = 222.6) which in ultraviolet region (λ = 400−10 nm). The plot of absorption coefficient spectrum $I(\omega)$, in Figure 6d started at 3.83 eV and its maximum arises at 23.30 eV at which maximum reflectivity occurs.

The maximum optical conductivity $\sigma(\omega)$ of 8560.9 $(\Omega cm)^{-1}$ was observed around 5.53 eV and also smaller conductivity peaks exist around 22.95 eV.

The electron energy loss function, $L(\omega)$, is a significant factor unfolding the energy loss of a fast electron passing through a material. The $L(\omega)$ shows two peaks, one broad peak at 13.1 eV and second highest principal spectral peak at 23.94 eV. The major peak in $L(\omega)$ represents the feature that is associated with plasma resonance, and the corresponding frequency is called plasma frequency, ω_p.[21] These peaks correspond to irregular edges in the reflectivity spectrum, and hence an abrupt reduction occurs at these peaks values in the reflectivity spectrum and it correlates with the zero crossing of $\varepsilon_1(0)$, shown in Figure 6f.

To the best of our knowledge, we first investigated the optical dispersions of perovskite-type $KMgH_3$. These properties may give insight related to their performance in applied fields and becomes motivation for the researcher to do more experiments in this direction.

4. CONCLUSIONS

In the present study, we have performed the first principles calculations of structural and elastic properties of $KMgH_3$ to search the stability of perovskite-type in three different phases, namely **US1**, **US2**, and **Stable** using FP-LAPW + lo method within a framework of the density functional theory. The electronic and optical properties were studied for only **Stable** perovskite-type $KMgH_3$. The structural parameters have been computed and found to be in good agreement with the existing experimental and theoretical data. The results of electronic charge density unveiled the bonding nature between K−H, K−Mg−H, and Mg−H in the light of electronegativity difference. The electronic band structure and density of states for $KMgH_3$ reveal that wide band gap arise due to H contribution at Fermi level. The optical parameters such as $\varepsilon(\omega)$, $n(\omega)$, $k(\omega)$, $R(\omega)$, $I(\omega)$, $\sigma(\omega)$ and $L(\omega)$ were also be calculated and analyzed and it was found an existence of Plasmon resonance at energies about 5.10 eV.

AUTHOR INFORMATION

Corresponding Author

*Tel: +420 777 729 583. Fax: +420-386 361 219. E-mail address:maalidph@yahoo.co.uk.

ACKNOWLEDGMENT

This work was supported from the institutional research concept of the Institute of Physical Biology, UFB (No. MSM6007665808), the program RDI of the Czech Republic, the project CENAKVA (No. CZ.1.05/2.1.00/01.0024), the Grant 152/2010/Z of the Grant Agency of the University of South Bohemia, and The School of Microelectronic Engineering, University Malaysia Perlis (UniMAP), Perlis, Malaysia. The PhD

student Yasir Saeed would like to thank the Institute of Physical Biology-University of South Bohemia for offering him the PhD position.

REFERENCES

(1) Park, H. H.; Pezat, M.; Darriet, B. *Rev. Chim. Min.* **1986**, *23*, 323.
(2) Park, H. H.; Pezat, M.; Darriet, B. *C. R. Acad. Sci.* **1988**, *306*, 963.
(3) Schumacher, R.; Weiss, A. *J. Less-Common Met.* **1990**, *163*, 179.
(4) Messer, C. E.; Eastman, J. C.; Mers, R. G.; Maeland, A. J. *Inorg. Chem.* **1964**, *3*, 776.
(5) Vajeeston, P.; Ravindran, P.; Kjekshus, A.; Fjellvåg, H. *J. Alloys Compd.* **2008**, *450*, 327.
(6) Zh., S.; Karazhanov, A. G.; Ulyashin, P.; Ravindran, P.; Vajeeston, E. P. L. *EPL* **2008**, *82*, 17006.
(7) *Encyclopedia of Inorganic Chemistry*; Yvon, K., King, R. B., Eds.; Wiley: New York, 1994; Vol. 3.
(8) Mamatha, A.; Bogdanovic, B.; Felderhoff, M.; Pommerin, A.; Schmidt, W; Schüth, F.; Weidenthaler, C. *J. Alloys Comp.* **2006**, *407*, 78.
(9) Ghebouli, B.; Ghebouli, M. A.; Fatmi, M. *Eur. Phys. J. Appl. Phys.* **2010**, *51*, 20302.
(10) Ghebouli, B.; Ghebouli, M. A.; Fatmi, M. *Solid State Sci.* **2010**, *12*, 587.
(11) Blaha, P.; Schwarz, K.; Madsen, G.K.H.; Kvanicka, D.; Luitz, J., 2001 *WIEN2K, An Augmented plane wave + Local Orbital Program for Calculating Crystal Properties Karlheinz Schwarz*; Techn. Universitat: Wien, Austria. ISBN: 3-9501031-1-1-2.
(12) Perdew, J. P.; Burke, K.; Ernzerhof, M. *Phys. Rev. Lett.* **1996**, *77*, 3865.
(13) Murnaghan, F. D. *Proc. Natl. Acad. Sci. U.S.A.* **1944**, *30*, 244.
(14) Mehl, M.J.; Papaconstantopoulos, D.A. *Phys. Rev. B* **1996**, *54*, 4519.
(15) Wallace, D. C. *Thermodynamics of Crystals*; Wiley: New York, 1972.
(16) Park, H.-H.; Pezat, M.; Darriet, B.; Hagenmuller, P. *J. Less-Common Met.* **1987**, *136*, 1.
(17) Klaveness, A.; Swang, O.; Fjellvåg, H. *Europhys. Lett.* **2006**, *76*, 285.
(18) Khan, M. A.; Kashyap, A.; Solanki, A. K.; Nautiyal, T.; Auluck, S. *Phys. Rev. B* **1993**, *23*, 16974.
(19) Wooten, F. *Optical properties of Solids*; Academic: New York, 1972.
(20) Penn, D. R. *Phys. Rev. B* **1962**, *128*, 2093.
(21) Anderson, O. L. *J. Phys. Chem. Solids* **1963**, *24*, 909.